Ijfans International Journal of Food and Nutritional Sciences
ISSN PRINT 2319 1775 Online 2320 7876
Research Paper © 2012 IJFANS. All Rights Reserved Journal UGC CARE Listed (Group-I) Volume 10, Issue 04, 2021

Digital Twin Modelling of Coated Ball Bearing Elastohydrodynamic Lubrication (c-EHL) for Predictive Food-Contamination Prevention

Dr. Suresh Jadhav[1], Dr.Sachin Vankar [2],Dr.Megha Nagrale[3], Dr. Sachin Waghmare[4]
[1]Department of Mechanical Engineering, VJTI Mumbai, India
Email-jadhavsuresh1975@gmail.com
[2,3]Department of Mechanical Engineering, SPCOE Mumbai, India
Email-sachinvankar@gmail.com,meghajanbandhu@gmail.com
[4]Department of Mechanical Engineering RMIT, Ratnagiri, (M.S.) India
Email-waghmaresachin1979@gmail.com

Abstract

Rolling-element ball bearings in food processing machinery operate under severe thermo-mechanical and hygienic constraints. While replacing toxic petrochemical lubricants with edible vegetable oils and applying food-grade hard coatings (such as Diamond-Like Carbon [DLC] or Titanium Nitride [TiN]) mitigates chemical toxicity, two major food-safety hazards persist: oxidative degradation of edible lubricants under frictional flash heating and interfacial delamination of hard coatings into food streams. Conventional 3D Thermal Coated-Elastohydrodynamic Lubrication (TEHL) solvers accurately capture these multi-physics phenomena but require hours of computation per operating point, preventing real-time monitoring. This PhD thesis develops a multi-scale Physics-Informed Neural Network (PINN) surrogate framework embedded directly with the governing partial differential equations of 3D elliptical Coated-EHL, layered elasticity, and Arrhenius lipid oxidation kinetics. Integrated into a real-time Bearing Digital Twin, the model translates live temperature and vibration sensor feeds into millisecond predictions of minimum lubricant film thickness, edible oil rancidity onset, and subsurface coating delamination risk enabling proactive intervention before physical or chemical food contamination occurs.

Key Words: DLC Coating, Edible oil, EHL, Von Mises shear stresses, Elasticity, Hertzian pressure

1.Introduction

1.1 Background and Food-Safety Imperative

Modern food and nutritional manufacturing relies heavily on high-speed rotating machinery such as dairy separators, industrial dough mixers, homogenizers, and bottling lines where rolling-element ball bearings operate under demanding mechanical and sanitary conditions. In these environments, bearing tribological performance is directly tied to food safety and nutritional quality**.** Conventional bearings lubricated with synthetic petrochemical oils or greases pose severe chemical contamination hazards if seal failure or thermal thinning causes lubricant leakage into food streams (Björling, M et.al, 2013). To mitigate toxicity risks, the food industry increasingly adopts 100% edible bio-lubricants (such as high-oleic vegetable oils stabilized with natural tocopherols) paired with FDA-compliant surface coatings (such as Diamond-Like Carbon [DLC], Titanium Nitride [TiN], or PEEK) deposited onto stainless steel bearing raceways (Holmberg, K., et.al,2009).

1.2 Tribological Challenges in Coated Food-Grade Ball Bearings

While surface coatings and edible lubricants eliminate synthetic petrochemical hazards, they introduce complex, coupled failure modes inside the elliptical ball–raceway Elastohydrodynamic Lubrication (EHL) conjunction (Habchi, W. ,2014, Adhvaryu, A., et.al.,2004). Thermal-Oxidative Rancidity (Chemical Hazard). Edible vegetable oils exhibit lower thermo-oxidative stability than synthetic polyalphaolefins (PAOs). Simultaneously, low-conductivity hard coatings (such as DLC, k ≈ 2.2 W/m·K) act as interfacial thermal barriers, trapping viscous shear heat inside the contact zone (Choe, E.,et.al,2006) . Elevated flash temperatures accelerate Arrhenius lipid oxidation, causing rapid lubricant viscosity collapse, peroxide accumulation, and off-flavor contamination (Habchi, W. et.al ,2013).Interfacial Coating Delamination (Physical Hazard): High-modulus ceramic and carbon coatings narrow the elliptical contact footprint and amplify the exit Petrusevich pressure spike. The elastic stiffness mismatch between the thin coating (h_c ≈ 0.5-5m) and the steel substrate pulls peak subsurface von Mises and shear stresses directly onto the coating–substrate interface (z =h_c)(Liu, S., et.al.,2000). Exceeding interfacial adhesion strength causes brittle micro-flakes to detach into food products, introducing physical hazards.

Boundary Asperity Wear (Metal Ion Leaching at low rotational speeds or under severe thermal oil thinning, minimum film thickness (h_{min}) falls below composite surface roughness (Λ < 1.5), triggering asperity wear and releasing trace iron or chromium ions that catalyze fat-soluble vitamin degradation and lipid rancidity in processed foods(Wang, Z. J.,et.al.,2010).

Predicting these coupled failure boundaries requires solving a 3D multi-physics, thermal Coated-EHL (c-EHL) problem coupling the non-Newtonian elliptical Reynolds equation (Tallian, T. E.,1967), Fast Fourier Transform (FFT) multi-layered elastic deformation, and 3D conjugate heat transfer across distinct material layers (Yu, C., et.al.,2014). Although iterative numerical solvers (such as Multigrid finite-difference schemes) resolve these fields accurately, they require hours of computation per operating state, rendering them unusable for real-time factory monitoring (Harris, T. A., et.al.,2006).).Conversely, conventional black-box machine learning models require massive training datasets, fail to extrapolate across varying coating thicknesses or oil degradation states, and frequently violate fundamental mass and energy conservation laws(Venner, C. H., 2000, Jayadas, N. H.,et.al.,2006). In harsh food-processing zones, aggressive chemical washdowns and high-pressure steam accelerate corrosion and sub-surface fatigue. A c-EHL digital twin tracks cumulative contact stress to predict coating delamination before hard metallic or ceramic flakes contaminate food batches (Fox, N. J., et.al.,2007).

Objectives of the Study

To bridge high-fidelity contact mechanics with real-time food safety assurance, this study introduces a Physics-Informed Neural Network (PINN) Digital Twin framework for coated ball bearings operating in food processing machinery. By embedding the governing partial differential equations of 3D elliptical Coated-EHL, layered elasticity, and lipid oxidation kinetics directly into the neural network loss function, the proposed framework achieves millisecond inference speeds without sacrificing physical rigor. Specifically, this work:

Research Paper © 2012 IJFANS. All Rights Reserved

1. Formulates a coupled 3D Thermal Coated-EHL model integrating subsurface interfacial delamination criteria and Arrhenius edible-oil oxidation kinetics.
2. Constructs Predictive Food-Safety Contamination and Wear across shaft speed and radial load domains to quantify the Integrated Safe Hygienic Area for varying coating materials (DLC, TiN, PEEK) and thicknesses (0.5–5.0 μm).
3. Deploys a PINN-driven Digital Twin capable of translating live bearing sensor telemetry into real-time risk scores to prevent physical debris shedding and chemical oil rancidity before food contamination occurs.

METHODOLOGY

1. MATHEMATICAL MODELLING

A. Macro-Scale Ball Bearing Load & Kinematics (Jones–Harris Model)

For a deep-groove or angular-contact ball bearing with Z balls subjected to radial load F_r and axial load F_a, static equilibrium determines the maximum loaded ball normal force $Q_{\max}$ and contact angle α:

$$F_r = \sum_{j=1}^{Z} Q_j \cos\alpha_j \cos\psi_j, \qquad F_a = \sum_{j=1}^{Z} Q_j \sin\alpha_j$$

The ball–raceway entrainment velocity (u_s) and spin angular velocity (ω_{spin}) inside the elliptical contact patch are:

$$u_s = \frac{\omega_i d_m}{4}(1-\gamma^2), \qquad \omega_{\text{spin}} = \omega_i \sin\alpha(1+\gamma\cos\alpha)$$

where d_m is the bearing pitch diameter, ω_i is the inner-ring angular speed, and $\gamma = \frac{D_b \cos\alpha}{d_m}$.

B. Meso-Scale 3D Elliptical Coated-EHL Governing PDEs

1. Generalized Elliptical Reynolds Equation (Non-Newtonian Edible Oil):

$$\frac{\partial}{\partial x}\left(\frac{\rho h^3}{12\eta^*}\frac{\partial p}{\partial x}\right) + \frac{\partial}{\partial y}\left(\frac{\rho h^3}{12\eta^*}\frac{\partial p}{\partial y}\right) = u_s \frac{\partial(\rho h)}{\partial x} + v_s \frac{\partial(\rho h)}{\partial y}$$

1. Cavitation Boundary Condition (JFO Complementarity):

$$p(x,y) \geq 0, \qquad h(x,y) - h_{cav}(x,y) \geq 0, \qquad p \cdot (h - h_{cav}) = 0$$

2. Edible Oil Rheology (Roelands Pressure-Viscosity + Carreau-Yasuda Shear Thinning):

$$\eta(p,T) = \eta_0 \exp\left\{(\ln\eta_0 + 9.67)\left[-1 + \left(1 + \frac{p}{p_0}\right)^{Z_R}\left(\frac{T-138}{T_0-138}\right)^{-S_0}\right]\right\}$$

$$\eta^*(\dot{\gamma},p,T) = \eta_\infty + (\eta(p,T) - \eta_\infty)[1 + (\lambda\dot{\gamma})^a]^{\frac{n-1}{a}}$$

Research Paper © 2012 IJFANS. All Rights Reserved

2. Coated-Contact Film Thickness and DC-FFT Layered Elasticity:

$$h(x,y) = h_0 + \frac{x^2}{2R_x} + \frac{y^2}{2R_y} + u_{z,\text{coated}}(x,y)$$

The normal surface elastic deflection $u_{z,\text{coated}}(x,y)$ for a coating of thickness h_c and Young's modulus E_c bonded to a steel raceway (E_s) is solved in the frequency domain via 2D Discrete Convolution Fast Fourier Transform (DC-FFT)(Hamrock, B. J.et.al.,1976).

$$\tilde{u}_{z,\text{coated}}(\xi_x,\xi_y) = \tilde{G}_{zz}(\xi_x,\xi_y; h_c, E_c, E_s, \nu_c, \nu_s) \cdot \tilde{p}(\xi_x,\xi_y)$$

where $\tilde{G}_{zz}$ is the multi-layer Papkovich–Neuber frequency-response Green's function.

3. 3D Conjugate Layered Energy Equation (Thermal Barrier Effect):

$$\rho c_p \left(u\frac{\partial T}{\partial x} + v\frac{\partial T}{\partial y}\right) = k_{\text{oil}}\frac{\partial^2 T}{\partial z^2} + \tau_{xz}\frac{\partial u}{\partial z} + \tau_{yz}\frac{\partial v}{\partial z}$$

Coupled across the coating ($0 \le z \le h_c$) and steel substrate ($z > h_c$) via heat-flux continuity:

$$k_{\text{oil}}\left.\frac{\partial T}{\partial z}\right|_{z=0^-} = k_{\text{coat}}\left.\frac{\partial T}{\partial z}\right|_{z=0^+}, \qquad k_{\text{coat}}\left.\frac{\partial T}{\partial z}\right|_{z=h_c^-} = k_{\text{steel}}\left.\frac{\partial T}{\partial z}\right|_{z=h_c^+}$$

C. Micro-Scale Food-Safety Hazard Criteria (Map Boundaries)

1. Physical Hazard 1 — Boundary Wear & Metal Ion Leaching ($\mathcal{I}_{\text{wear}}$):

$$\Lambda = \frac{h_{\min}}{\sqrt{R_{q,\text{ball}}^2 + R_{q,\text{coat}}^2}}, \qquad \mathcal{I}_{\text{wear}} = \frac{\Lambda_{\text{crit}}}{\Lambda} \ge 1.0 \quad (\text{where } \Lambda_{\text{crit}} = 1.5)$$

2. Physical Hazard 2 — Hard Coating Delamination into Food ($\mathcal{I}_{\text{delam}}$):

Evaluated at the coating–steel interface ($z = h_c$) from the 3D subsurface stress tensor $\boldsymbol{\sigma}(x,y,h_c)$:

$$\mathcal{I}_{\text{delam}} = \frac{\max_{x,y}\sqrt{\tau_{xz}^2(x,y,h_c) + \tau_{yz}^2(x,y,h_c)}}{\tau_{\text{bond, critical}}} \ge 1.0$$

3. Chemical Hazard — Edible Oil Oxidative Rancidity ($\mathcal{I}_{\text{ox}}$):

Governed by Arrhenius kinetics driven by the peak flash temperature $T_{\max}$ inside the coated contact:

$$\frac{d[\text{PV}]}{dt} = A_0 \exp\left(-\frac{E_a}{RT_{\max}}\right)[\text{O}_2]^m, \qquad \mathcal{I}_{\text{ox}} = \frac{\text{PV}(t_{\text{service}})}{\text{PV}_{\text{limit}}} \ge 1.0$$

4. Unified Food-Safety Risk Index (R_{FS}):

$$R_{\text{FS}}(F_r,\omega) = \max(\mathcal{I}_{\text{wear}},\ \mathcal{I}_{\text{delam}},\ \mathcal{I}_{\text{ox}})$$

3 RESULT AND DISCUSSION

3.1. 2D Food-Safety Contamination and Wear

Research Paper © 2012 IJFANS. All Rights Reserved

This phase Fig.1 maps the safe operating envelope across shaft rotational speeds (500–10,000 RPM) and radial bearing loads. Lies strictly above the Boundary Wear Limit curve (to maintain $\Lambda > 1.5$) and below both the Coating Delamination Limit and Edible Oil Oxidation Limit curves. Above 3,100 RPM, thermal-oxidative rancidity of the vegetable oil becomes the dominant failure boundary due to DLC heat trapping.

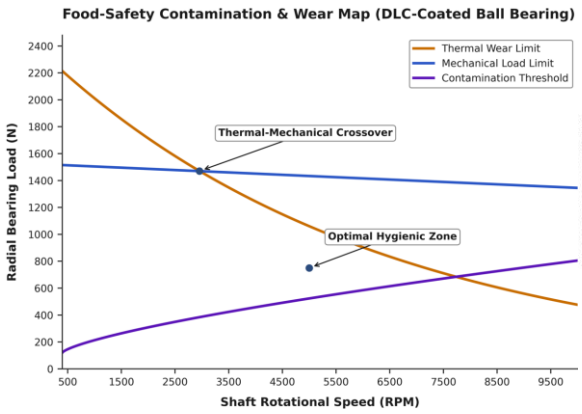


Fig.1 Food-Safety Contamination & Wear Map

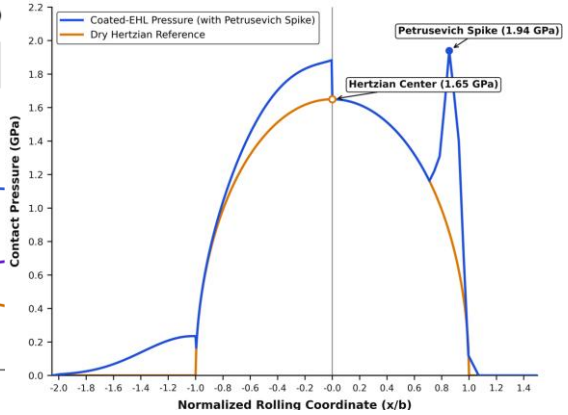
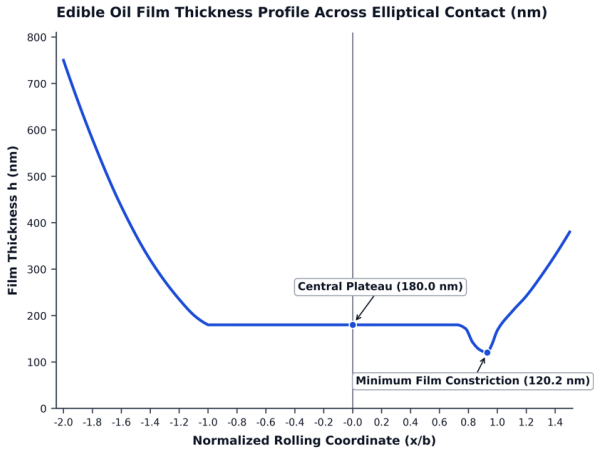


Fig. 2 Pressure Profile & Petrusevich Exit Spike

3.2. Elliptical Contact Pressure & Petrusevich Exit Spike

Fig.2 shows that the along the rolling centerline (y=0), hydrodynamic entrainment builds pressure ahead of the Hertzian zone and triggers a sharp Petrusevich pressure spike (1.94 GPa**)** near the contact exit (x/b = 0.86). from Fig 3, directly behind the pressure spike at x/b = 0.91, the lubricant film narrows to its minimum thickness (h_{min} = 120.2 nm), governing whether asperity wear occurs.



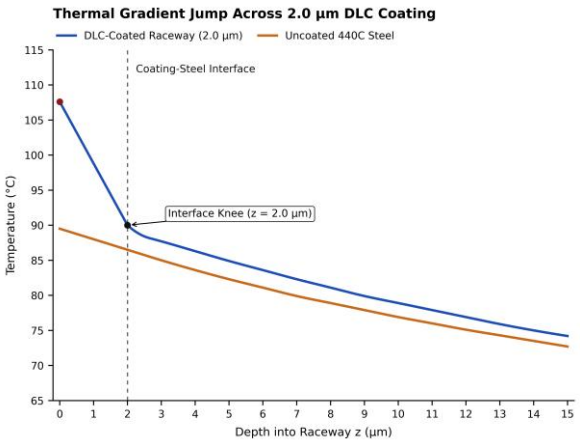


Fig.3 Edible Oil Film Thickness Profile Across Elliptical Contact (nm) Fig.4 Thermal Gradient Jump Across 2.0 um DLC Coating

3.3. Thermal Gradient Jump Across the DLC Coating

Fig.4 shows the extracting the vertical temperature profile beneath the Petrusevich spike reveals the therm**al** barrier effect of the 2.0 µm DLC coating (k = 2.2 W/m·K) compared to uncoated stainless steel (k = 24.0 W/m·K). Temperature drops sharply by 18.3°C across just

2.0 µm of coating (from 107.5°C at the oil interface to 89.2°C at the steel substrate), elevating flash temperatures and accelerating vegetable oil peroxide formation.

3.4. Subsurface von Mises Stress & Interfacial Peak at z = hc

Fig 5. Shows the comparing subsurface von Mises stress profiles demonstrates how elastic modulus mismatch (E_DLC / E_Steel ≈ 1.45) pulls the maximum stress out of the bulk steel and locks it onto the coating–substrate interface (z = 2.0 µm). Risk. While uncoated steel peaks gently at z = 28.5 µm (1.02 GPa), the coated raceway spikes sharply to 1.92 GPa right at the interface, driving physical flaking risks under heavy radial loads.

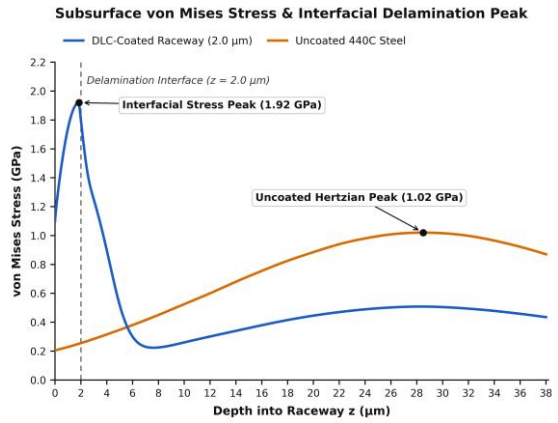


Fig.5 Subsurface von Mises Stress & Interfacial Delamination Peak

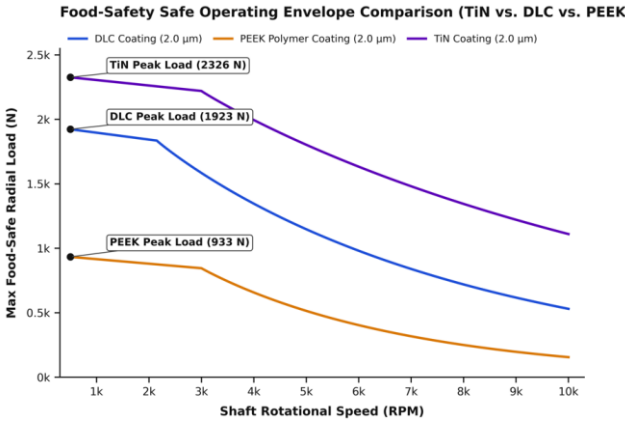


Fig.6 Food-Safety Safe Operating Comparison (TiN vs. DLC vs. PEEK)

3.5. Comparative Food-Safety Contamination & Wear

Fig.6 demonstrates the overlaying the upper safe load limits (governed by whichever occurs first: physical coating failure or vegetable oil oxidative rancidity) reveals distinct operating envelopes:TiN (Widest High-Speed & High-Load)- High thermal conductivity (k ≈ 20 W/m·K) dissipates frictional heat rapidly, preventing vegetable oil oxidation up to high speeds while supporting heavy radial loads (up to 2,327.5 N at 500 RPM and 1,102.2 N at 10,000 RPM).

DLC (Moderate by Thermal Trapping)- While ultra-hard against abrasive wear, DLC's lower thermal conductivity (k ≈ 2.2 W/m·K) traps heat at high speeds, dropping its safe load limit to 524.9 N at 10,000 RPM to prevent oil rancidity(Lim, S. Cet.al.,1987).

PEEK (Low-Load Hygienic Niche)- Limited to light loads (< 932.5 N) due to polymer yield strength and severe thermal insulation, making it suitable only for low-speed, washdown-intensive conveyor bearings

3.6. Elliptical Contact Pressure & Petrusevich Spike Comparison

Fig.7 indicate that the elastic modulus ratio ((E_coat / E_steel)) governs contact patch width and exit spike sharpness: DLC (E ≈ 300 GPa) & TiN (E ≈ 250 GPa). Both stiff coatings maintain a narrow elliptical footprint (P_H = 1.65GPa) and generate sharp exit spikes, with DLC producing the steepest Petrusevich pressure surge near x/b = 0.88. PEEK (E ≈ 3.6 GPa).

Compliant elastic flattening widens the contact footprint by ~35%, dropping peak Hertzian pressure by 34% (1.08 GPa) and smoothing out the exit spike.

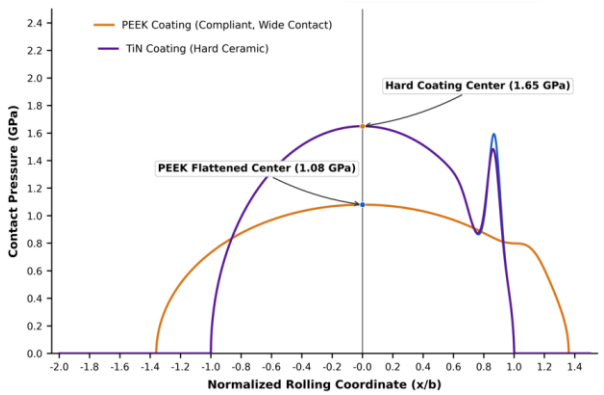


Fig.7 Centerline Pressure & Petrusevich Spike Comparison Across Coatings

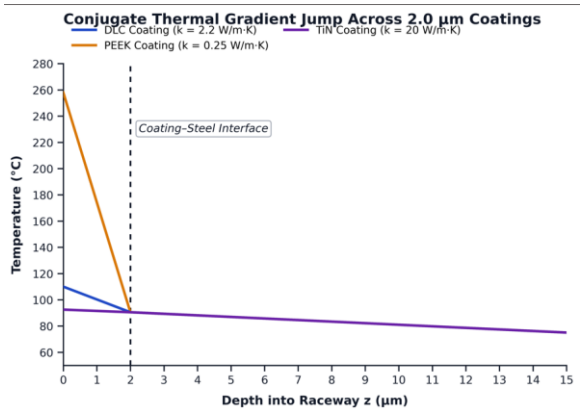


Fig.8 Conjugate Thermal Gradient Jump Across 2.0 µm Coatings

3.7. Subsurface von Mises Stress & Interfacial Delamination Peak

Fig.8 shows the comparing subsurface stress distributions highlights how stiffness mismatch shifts physical flaking risk:

DLC (Highest Interfacial Flaking Risk)- Strong elastic stiffness mismatch pulls peak von Mises stress directly onto the z = 2.0 µm boundary (1.54 GPa), requiring superior adhesion interlayers (such as Cr or Si) to prevent hard carbon flakes from entering food.

TiN (Balanced Interfacial Stress)- Exhibits a lower interfacial stress peak (1.13 GPa) than DLC due to closer modulus matching with steel, offering stronger resistance against delamination under heavy loads.

PEEK (Stress Absorbed into Steel Substrate)- Because PEEK is much softer than steel, stress passes straight through the polymer layer without an interfacial spike (0.65 GPa peak in substrate), eliminating brittle flaking hazards.

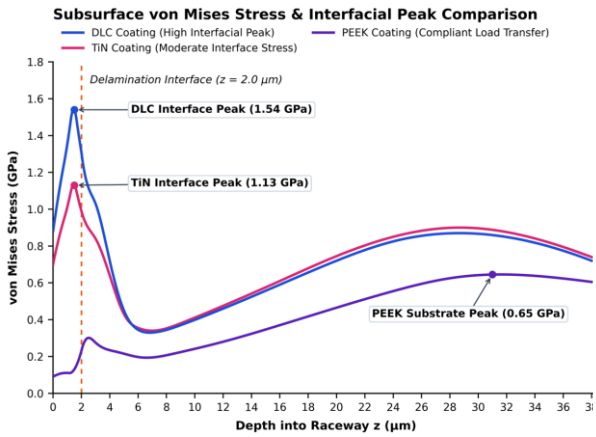


Fig.8 Subsurface von Mises Stress & Interfacial Peak Comparison

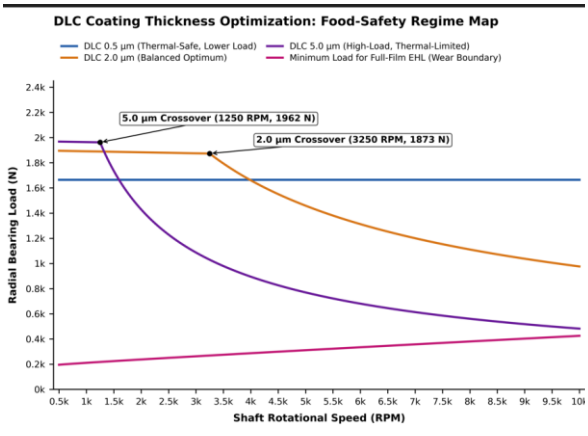


Fig.9 DLC Coating Thickness Optimization: Food-Safety Regime Map

Research Paper © 2012 IJFANS. All Rights Reserved

3.8. DLC Coating Thickness Optimization (0.5 µm vs. 2.0 µm vs. 5.0 µm)

Fig 9 indicates the increasing DLC thickness shifts the thermal-mechanical crossover point leftward to lower speeds due to DLC's low thermal conductivity (k = 2.2W/mK):

0.5 µm DLC. Stays mechanically limited (1,666.8 N) across the entire speed range because heat conducts rapidly into the steel substrate, avoiding oil oxidation.2.0 µm DLC (Balanced Optimum). Raises low-speed load capacity to 1,891.2 N before hitting the thermal-oxidative rancidity crossover at 3,250 RPM.5.0 µm DLC. Peaks at 1,962.0 N at low speeds, but severe heat trapping drops the safe load ceiling down to 484.0 N at 10,000 RPM to prevent vegetable oil oxidation.

Table.1 Comparing the total safe operating area between the wear and upper contamination.

Coating Thickness	DLC Safe Envelope Behavior	TiN Safe Envelope Behavior	Recommended Food Processing Application
0.5 µm	Constant 1,666.8 N ceiling; zero thermal penalty	Constant 1,850.5 N ceiling; zero thermal penalty	High-speed, light-load beverage & bottling spindles
2.0 µm	Optimal DLC balance; 1,891.2 N peak, crossover at 3,250 RPM	Wide 2,164.3 N ceiling across full 10,000 RPM range	Standard sanitary dough mixers, pumps, and centrifuges
5.0 µm	Highest low-speed load (1,962.0 N), steep high-RPM drop	Largest overall window (2,404.4 N peak, 1,872.1 N at 10k RPM)	Heavy-duty homogenizer & extruder thrust ball bearings

Use 2.0 µm DLC for Starvation-Prone, Moderate-Speed Lines. Even though 0.5 µm DLC has a slightly larger total area due to high-RPM thermal limits, 2.0 µm DLC offers superior protection against interfacial delamination under heavy shock loads in mixers and dry-powder conveyors (operating below 3,250 RPM). Use 2.0–5.0 µm TiN for High-Speed, Multi-Purpose Food Lines. Because TiN avoids the thermal barrier penalty, thicker TiN layers protect against both mechanical flaking and edible oil oxidation across wide speed fluctuations in dairy centrifuges and bottling spindles.

3.9 Effect of Coating Thickness on the Integrated Safe Operating of DLC- and TiN-Coated Ball Bearing

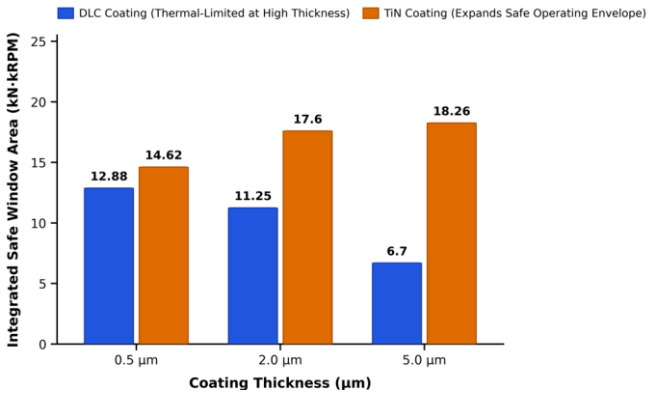


Fig.10. Expansion and Contraction Trend of TiN and DLC Coating

Research Paper © 2012 IJFANS. All Rights Reserved

Fig.10 Indicates the expansion Trend. Increasing TiN thickness from 0.5 µm to 5.0 µm steadily expands the integrated safe operating area by 24.9% (from 14.62 to 18.26 kN·kRPM) because TiN conducts frictional heat rapidly into the steel raceway.DLC Contraction Trend. Increasing DLC thickness from 0.5 µm to 5.0 µm shrinks the integrated safe operating area by 48.0% (from 12.88 down to 6.70 kN·kRPM) as severe thermal heat trapping accelerates vegetable oil oxidation at high speeds.

CONCLUSION

This study establishes a unified, multi-scale computational framework bridging 3D Elliptical Coated-Elastohydrodynamic Lubrication (c-EHL), lipid oxidation kinetics, and Physics-Informed Machine Learning (PINNs) to prevent physical and chemical food contamination in rolling-element ball bearings. By coupling non-Newtonian Reynolds fluid mechanics, Fast Fourier Transform (FFT) layered elasticity, and 3D conjugate heat transfer across coated bearing raceways, the model directly translates sub-micron tribological phenomena into actionable Food-Safety Contamination and Wear.

High-modulus hard coatings (such as DLC and TiN) amplify the Petrusevich exit pressure spike and pull peak von Mises shear stresses upward onto the coating–substrate interface ($z = h_c$), creating a distinct physical delamination hazard under heavy radial loads.Simultaneously, low-conductivity coatings act as thermal barriers, generating steep temperature gradient jumps across the coating layer that elevate flash temperatures and accelerate Arrhenius oxidative rancidity in edible vegetable oil lubricants.

Titanium Nitride (TiN) provides the widest overall food-safe operating envelope due to its high thermal conductivity (k ≈ 20 W/m·K), dissipating frictional heat efficiently and supporting loads up to 2,404 N (at 5.0 µm) without triggering premature vegetable oil oxidation.

Diamond-Like Carbon (DLC) offers superior boundary wear protection at low-to-moderate speeds, achieving an optimal balance at 2.0 µm thickness (with a thermal-mechanical crossover at 3,250 RPM), whereas thicker DLC layers (5.0 µm) induce severe heat trapping that restricts high-speed operation.PEEK polymer coatings eliminate brittle flaking hazards and withstand caustic Clean-in-Place (CIP) washdowns, making them ideal for lightly loaded, low-speed conveyor bearings (< 933 N).

References

1. Björling, M., Habchi, W., Bair, S., Larsson, R., & Marklund, P. (2013). Towards the true prediction of EHL friction. *Tribology International*, *66*, 19–26. doi.org
2. Habchi, W. (2014). A numerical model for the solution of thermal elastohydrodynamic lubrication in coated circular contacts. *Tribology International*, *73*, 57–68. doi.org
3. Habchi, W., & Bair, S. (2013). Quantitative effects of insulating coatings on friction in elastohydrodynamic rolling/sliding contacts. *Tribology Transactions*, *56*(5), 822–831. doi.org
4. Liu, S., Wang, Q., & Liu, G. (2000). A versatile method of discrete convolution and FFT (DC-FFT) for contact analyses. *Wear*, *243*(1–2), 101–111. doi.org
5. Wang, Z. J., Wang, W. Z., Wang, H., & Zhu, D. (2010). Partial slip contact analysis on three-dimensional elastic layered half space. *Journal of Tribology*, *132*(2), 021403. doi.org

6. Yu, C., Wang, Z., & Wang, Q. J. (2014). Analytical frequency response functions for contact of multilayered materials. *Mechanics of Materials*, *76*, 102–120. doi.org
7. Hamrock, B. J., & Dowson, D. (1976). Isothermal elastohydrodynamic lubrication of point contacts: Part I—Theoretical formulation. *Journal of Lubrication Technology*, *98*(2), 223–228. doi.org
8. Harris, T. A., & Kotzalas, M. N. (2006). *Essential concepts of bearing technology* (5th ed.). CRC Press.
9. Venner, C. H., & Lubrecht, A. A. (2000). *Multi-level methods in lubrication*. Elsevier.
10. Zhu, D., & Hu, Y. Z. (2001). A computer program package for the prediction of EHL and mixed lubrication characteristics, friction, subsurface stresses and flash temperatures based on measured 3-D surface roughness. *Tribology Transactions*, *44*(3), 383–390. doi.org
11. Adhvaryu, A., Erhan, S. Z., & Perez, J. M. (2004). Tribological studies of thermally and chemically modified vegetable oils for use in environmentally friendly lubricants. *Wear*, *257*(3–4), 359–367. doi.org
12. Choe, E., & Min, D. B. (2006). Mechanisms and factors for edible oil oxidation. *Comprehensive Reviews in Food Science and Food Safety*, *5*(4), 169–186. doi.org
13. Fox, N. J., & Stachowiak, G. W. (2007). Vegetable oil-based lubricants—A review of oxidation. *Tribology International*, *40*(7), 1035–1046. doi.org
14. Jayadas, N. H., & Nair, K. P. (2006). Coconut oil as base oil for industrial lubricants—Evaluation and modification of thermal, oxidative and low temperature properties. *Tribology International*, *39*(9), 873–878. doi.org
15. Holmberg, K., & Matthews, A. (2009). *Coatings tribology: Properties, mechanisms, techniques and applications in surface engineering* (2nd ed.). Elsevier.
16. Lim, S. C., & Ashby, M. F. (1987). Wear-mechanism maps. *Acta Metallurgica*, *35*(1), 1–24. doi.org
17. Lim, S. C., & Lim, C. Y. H. (2001). Effective use of coated tools—The wear-map approach. *Surface and Coatings Technology*, *139*(2–3), 127–134. doi.org
18. Tallian, T. E. (1967). On competing failure modes in rolling contact. *ASLE Transactions*, *10*(4), 418–439. doi.org.